Macromolecular Research, Vol. 15, No. 7, pp 623-632 (2007)

# Preparation and Characterization of Nanoparticles Using Poly(*N*-isopropylacrylamide)-Poly(ε-caprolactone) and Poly(ethylene glycol)-Poly(ε-caprolactone) Block Copolymers with Thermosensitive Function

**Changyong Choi, Mi-Kyeong Jang, and Jae-Woon Nah***

*Department of Polymer Science and Engineering, Sunchon National University, Suncheon 540-742, Korea*

*Received June 18, 2007; Revised October 8, 2007*

**Abstract:** Thermosensitive nanoparticles were prepared via the self-assembly of two different poly(ε-caprolactone)-based block copolymers of poly(*N*-isopropylacrylamide)-*b*-poly(ε-caprolactone) (PNPCL) and poly(ethylene glycol)-*b*-poly(ε-caprolactone) (PEGCL). The self-aggregation and thermosensitive behaviors of the mixed nanoparticles were investigated using $^1$H-NMR, turbidimetry, differential scanning microcalorimetry (micro-DSC), dynamic light scattering (DLS), and fluorescence spectroscopy. The copolymer mixtures (mixed nanoparticles, M1-M5, with different PNPCL content) formed nano-sized self-aggregates in an aqueous environment via the intra- and/or intermolecular association of hydrophobic PCL chains. The microscopic investigation of the mixed nanoparticles showed that the critical aggregation concentration (cac), the partition equilibrium constants ($K_v$) of pyrene, and the aggregation number of PCL chains per one hydrophobic microdomain varied in accordance with the compositions of the mixed nanoparticles. Furthermore, the PNPCL harboring mixed nanoparticles evidenced phase transition behavior, originated by coil to the globule transition of PNiPAAm block upon heating, thereby resulting in the turbidity change, endothermic heat exchange, and particle size reduction upon heating. The drug release tests showed that the formation of the thermosensitive hydrogel layer enhanced the sustained drug release patterns by functioning as an additional diffusion barrier.

*Keywords*: nanoparticles, thermosensitive, PCL, PNiPAAm, PEG, drug delivery.

## Introduction

Block copolymers, containing hydrophobic and hydrophilic chains, have been studied in biotechnology and pharmaceutical fields for their unique properties forming micelle or micelle-like self-aggregate in aqueous milieu.[1-3] In particular, polymeric micelles have been considered as one of the promising candidates for drug delivery systems owing more to the increment of drug concentration in an aqueous milieu than to the solubility limit of the hydrophobic free drug by partitioning the drugs into the hydrophobic core.[1-6]

The hydrophilic corona also endowed the polymeric self-aggregates with excellent physiological stabilities and biocompatibilities.[7-9] Therefore, a number of studies have focused on the applications of the polymeric self-aggregates into drug delivery systems.[10-15] As polymeric materials for the self-aggregate, amphiphilic block copolymers, hydrophobically modified water-soluble polymers, and hydrophobized polysaccharides have been extensively studies.[16-20]

Poly(ethylene glycol) (PEG), the hydrophilic corona, endowed the polymeric micelles with escape from nonspecific uptake by reticuloendothelial systems (RES). In the systemic circulation, the RES plays a crucial role for clearance of colloidal particle from the blood stream. Therefore, long systemic circulation can be achieved by introducing the PEG component into polymeric micelle systems.[9,21] Coupled with the long circulation effect, remarkably low critical micelle concentration is guaranteed to the polymeric micelle excellent stability owing to the rate of micelle dissociation slower than small molecular surfactant micelles during the systemic circulation. Furthermore, the enhanced permeation and retention effect at a tumor site gave the possibility of passive targeting of the polymeric micelles into tumor site.[22,23]

Although numerous studies and promising results of the polymeric self-aggregates as drug carriers have been reported, only few researches have been focus on the stimuli responsive polymeric nanoparticles. One of the most widely investigated stimuli sensitive polymers are poly(*N*-isopropylacrylamide) (PNiPAAm) and related copolymers.[24-28] Owing to the amphiphilic characters in the monomeric unit, the PNiPAAm shows unique reversible thermosensitivity with

*Corresponding Author. E-mail: jwnah@sunchon.ac.kr

the hydrated extended coil to globule transition by increasing temperature over its lower critical solution temperature (LCST). The LCST of PNiPAAm in aqueous environment is around 32 °C and is dependent on its molecular weight and incorporated comonomers.[29-31] Therefore, the PNiPAAm based several block copolymers have been studied as temperature sensitive polymeric nanoparticles.[32-38]

In this study, thermosensitive nanoparticles were prepared by self assembly of two different poly(ε-caprolactone) based block copolymers of poly(*N*-isopropylacrylamide)-*b*-poly(ε-caprolactone) (PNPCL) and poly(ethylene glycol)-*b*-poly(ε-caprolactone) (PEGCL). The hydrophobic block of PCL is well-known biodegradable polyester with excellent biocompatibility and degradability. Although a number of studies of PCL based amphiphilic block copolymers have well documented for the synthesis and characterization,[39-44] and application for drug delivery system (DDS), but the microscopic physicochemical properties of the block copolymers with different hydrophilic/hydrophobic balances still remain unclear. The self-aggregation and thermosensitive behaviors of the mixed nanoparticles (with different PNPCL content) were investigated by using $^1$H-NMR, turbidimetry, differential scanning microcalorimetry (micro-DSC), dynamic light scattering (DLS), and fluorescence spectroscopy. Finally, the efficacies of the mixed nanoparticles as drug carriers were examined with the hydrophobic model drug of clonazepam.

## Experimental

**Materials.** *N*-isopropylacrylamide monomer (NiPAAm), 2-mercaptoethanol (ME), 2,2'-azobisisobutyronitrile (AIBN), stannous 2-ethyl hexanoate (SnOct), pyrene, cetylpyridinium chloride (CPC), ε-caprolactone, and mPEG (MW 2,000) were purchased from Aldrich chemical Co.. The NIPAAm and mPEG were recrystallized in *n*-hexane and dichloromethane/diethyl ether system, respectively. The ε-caprolactone monomer was dried using $CaH_2$ and distilled under reduced pressure. The clonazepam (CNZ) was purchased from Sigma (St. Louis, MO) and used as received. All other chemicals and solvents were analytical or reagent grades and used without further purifications.

**Synthesis of Semitelechelic Poly(*N*-isopropylacrylamide) (PNiPAAm-OH).** Semitelechelic PNiPAAm with terminal hydroxyl group (PNiPAAm-OH) was synthesized by radical polymerization with 2-mercaptoethanol as a chain transfer agent and AIBN as an initiator. After dissolving the NiPAAm monomer (10 g, 88.4 m mole in 90 mL methanol), ME (0.372 g, 2.95 m mole) and AIBN (0.2 g) in methanol, the reaction mixture was degassed under reduced pressure by freeze-thawing cycles. Then the reaction mixture was transferred into thermostat bath at 70 °C and the polymerization was carried out for 24 h with vigorous stirring. After polymerization, the reaction solvent was removed using rotary evaporator. Finally, the polymer was dissolved in dichloromethane and precipitated in excess amount of diethyl ether. The precipitates were collected by filtration and washed with diethyl ether and dried *in vacuo* for 48 h. The dried polymer was dissolved in deionized water and fractionated by ultrafiltration with 10,000 and 3,000 molecular weight cut-offs membranes (ultrafiltration stirred cell, Amicon YM10, and YM3 membranes) at 4 °C. Each fractionated parts (> 10,000 and 3,000-10,000 fractions) were collected and freeze dried. Molecular weights of the PNiPAAms were determined by gel permeation chromatography and $^1$H-NMR end group analysis.

**Synthesis of PNPCL and PEGCL Block Copolymers.** PNPCL and PEGCL block copolymers were synthesized by ring opening polymerization of ε-caprolactone using PNiPAAm-OH (with > 10,000 fraction) and mPEG-OH (MW 2,000) as initiators with trace amount of SnOct as a catalyst. Predetermined amount of PNiPAAm-OH (or mPEG-OH) and toluene/xylene co-solvent (12.5 mL toluene/g, and 5 mL xylene/g) were introduced into a flask and moisture impurities were removed by azeotropic drying with removal of toluene at 120 °C. After drying and cooling (~60 °C), one drop of SnOct (100 μL) and predetermined amount ε-caprolactone monomer were added. Then, the polymerization reaction was performed at 140 °C for 24 h with vigorous stirring. After reaction, the diblock copolymers were obtained by precipitation in excess diethyl ether and dried *in vacuo* for 48 h. The resulting block copolymers were characterized by $^1$H-NMR and GPC.

**Characterization of PNiPAAm-OH and Block Copolymers.** $^1$H nuclear magnetic resonance ($^1$H-NMR) spectra of the PNiPAAm-OH and diblock copolymers were recorded by using Bruker spectrometer operating at 400 MHz using $D_2O$ (for PNiPAAm-OH) and $CDCl_3$ (block copolymers) as solvents. Chemical shifts ($\delta$) were given in ppm using tetramethylsilane (TMS) as internal reference. Average molecular weights and their distribution of the PNiPAAm-OH and copolymers were measured by gel permeation chromatography (GPC, Waters) using THF as elution solvent with monodisperse polystyrene standards.

**Preparation of Mixed Nanoparticles.** Mixed nanoparticles of PNPCL, PEGCL block copolymers and their mixtures (wt% of PNPCL of 100 (M1), 75 (M2), 50 (M3), 25 (M4), and 0 (M5)) were prepared by solvent evaporation method. Briefly, copolymers and their mixtures were dissolving in THF (5 mg/mL). Polymer solutions were dropped in chilled deionized water (80 mL, final concentration of polymer; 0.25 mg/mL) with sonication using probe type ultrasonic-generator (80 W). Then, THF removed by evaporation under reduced pressure. After the nanoparticle formation, the solutions were concentrated using ultrafiltration with 30 kDa MWCO membranes. Finally, mixed nanoparticles were obtained by lyophilization. The core-shell type mixed nanoparticles were characterized by $^1$H-NMR with

adopting different locking solvents ($D_2O$ and $CDCl_3$).

**Lower Critical Solution Temperature (LCST) Measurement.** To measure lower critical solution temperatures (LCSTs) of PNiPAAm-OH and mixed nanoparticles prepared by PNPCL and PEGCL, two different methods of cloud point measurement (turbidimetry) and calorimetric method were employed.[26,27,33,35,37] Firstly, optical transmittance of aqueous PNiPAAm solutions (1 mg/mL in $H_2O$) and mixed nanoparticles (1 mg/mL in $H_2O$) at various temperatures (30-42 °C, 1 °C interval) were measured at 500 nm wavelength using UV-VIS spectrometer (UV-1601, Shimadzu). At each temperature, the samples were stabilized for 10 min before measurements. Values for the LCST of polymer solution and nanoparticles dispersions were determined at a temperature with a half of the optical transmittance between below and above transitions.

The hydrated extended coil to globule transition of PNiPAAm chain is concomitant with change of thermodynamic parameters such as enthalpy and entropy. The enthalpy change of PNiPAAm solution and the mixed nanoparticles during phase transition was investigated by differential scanning microcalorimetry (micro-DSC). Eight hundred $\mu$L samples (5 mg/mL in $H_2O$) were loaded into DSC cells and heat exchange during the transition were monitored in the temperature range of 10-70 °C with a heating rate of 1 °C/min. As a reference, the DSC cells containing 800 mL $H_2O$ was used for normalization of the heat exchange. The endothermic peak points measured by micro-DSC were employed transition temperature (LCST).

**Measurement of Dynamic Light Scattering (DLS).** Particle size and size distribution of mixed nanoparticles were investigated by dynamic light scattering (DLS) instrument. The DLS measurements were carried out using ELS-800 electro phoretic LS spectrophotometer (Otsuka Electronics Co.) equipped with an argon laser operating at 632.8 nm at various temperature (25, 30, 35, and 40 °C) with a fixed scattering angle of 90°. Before measurement, the nanoparticles were re-dispersed in deionized water (1 mg/mL), sonicated for 30 sec, and filtered through a 0.8 $\mu$m pore size filter. Measurements were carried out at higher concentration than the critical aggregation concentration (cac) obtained by fluorescence spectroscope. The hydrodynamic diameters of the mixed nanoparticles were calculated by the Stokes-Einstein equation, and the polydispersity factors represented as $\mu_2/\Gamma^2$ were evaluated form the cummulant method ($\mu_2$; second cumulant of the decay function, $\Gamma^2$; average characteristic line width).[45,46]

The shapes of the mixed nanoparticles were also characterized by DLS (Malvern Instrument LTD. Series 4700) with and argon ion laser system at 488 nm with a digital autocorrelator. The scattering angle varied form 30 to 150° at constant temperature of 25 °C.[46-48] The PEGCL block copolymer concentrations of the samples were 1 mg/mL in deionized water.

**Fluorescence Measurements (Pyrene).** The pyrene solution in acetone ($6 \times 10^{-5}$ M, prepared prior to use) was added to the deionized water to make a pyrene concentration of $1.2 \times 10^{-6}$ M, and the acetone was removed at reduced pressure at 40 °C for 2 h. This solution was mixed with block copolymer nanoparticles solutions to make copolymer concentration from 2.0 to $1 \times 10^{-5}$ mg/mL, resulting in a pyrene concentration of $6 \times 10^{-7}$ M. Pyrene fluorescence spectra were obtained by using spectrofluorophotometer (RF-5301PC, Shimadzu). The excitation and emission wavelengths were 336 and 390 nm, respectively.

The aggregation number of PCL block per one hydrophobic domain was determined by the steady state fluorescence quenching method with CPC as a pyrene fluorescence quencher.[49,50] In microheterogeneous systems such as aqueous self-aggregate solution of amphiphilic block copolymers, the decrease in the probe fluorescence intensity is dependent upon concentration of the quenching molecule in the system ([$Q$]). The steady state quenching data is widely accepted to fit in the quenching kinetics as follows.

$$\ln(I_0/I) = [Q]/[M] \quad (1)$$

where $I_0$ and $I$ are the fluorescence intensity with the absence and presence of a quencher, [$Q$] is the concentration of the quencher, and [$M$] is the concentration of hydrophobic microdomains in the solution. Therefore, the number of hydrophobic group (PCL blocks in this system) in a hydrophobic microdomain ($N_{PCL}$) can be calculated by eq. (2).

$$N_{PCL} = [\text{PCL block}]/[M] \quad (2)$$

**Drug Release Studies.** The CNZ loaded mixed nanoparticles (wt% of PNPCL of 100 (M1), 75 (M2), 50 (M3), 25 (M4), and 0 (M5)) were carried out as followed: 20 mg of mixtures was dissolved in 5 mL of THF and 4 mg of CNZ was added. The solution was stirred at room temperature. The solution was dropped in cool deionized water (80 mL, final concentration of polymer; 0.25 mg/mL) during sonic using probe type ultrasonic-generator, followed by evaporation of THF under reduced pressure. After the CNZ loaded nanoparticles were formed, the solutions were concentrated using ultrafilteration with 30,000 molecular weight cut-offs membranes and then filtered a 0.8 $\mu$m pore sized filter to remove large aggregates, and CNZ loaded nanoparticles were obtained by lyophilization.

To measure drug content, the CNZ loaded nanoparticles were dissolved in DMF (0.01 mg/mL). The solution was centrifuged and supernatant was taken for measurement of drug concentration using UV-VIS spectrophotometer at 322 nm. Drug contents and loading efficiency were calculated eqs. (3) and (4).

$$\text{Drug contents} = A/(A + B) \times 100 \quad (3)$$

Where, $A$ and $B$ are the weight of remained drug in the

nanoparticles and polymer weight, respectively.

$$\text{Loading efficiency} = C/D \times 100 \quad (4)$$

Where, $C$ and $D$ are the amount of remained drug in the nanoparticles and initial feeding amount of drug, respectively.

The release experiment *in vitro* was carried out as follow: 4 mg of CNZ-loaded nanoparticles was dispersed into 1 mL of Na-PBS (pH: 7.4, ion strength: 0.15 M), which was put into a dialysis membrane (MWCO: 12,000) and the membrane were immersed into vials with 30 mL Na-PBS. Then, the drug release tests were performed at two different temperatures (25 and 37 °C) with continuous shaking (shaking water bath, 100 rpm). During the drug release test, whole media was withdrawn and replaced with fresh buffer solution at selected time intervals in order to prevent the reach of saturation concentration of drug in the solution. The concentration of the released CNZ was determined by UV-VIS spectrometer.

## Results and Discussion

**Synthesis and Characterization of PNiPAAm-OH, PNPCL, and PEGCL.** The semitelechelic polymer of hydroxyl terminated PNiPAAm-OH and PNPCL or PEGCL block copolymers were synthesized by radical chain-transfer polymerization and ring-opening polymerization of ε-caprolactone, respectively, and the schematic procedure of the polymerizations were illustrated in Figure 1.

Hydroxyl terminated PNiPAAm-OH was successfully synthesized by chain-transfer polymerization using 2-mercaptoethanol (ME) as chain transfer agent. However, the resulting polymer showed broad molecular weight distribution due to the uncertainty of the chain transfer polymerization. To minimize the unwanted side effect such as increasing LCST by low molecular weight portions, low molecular weight impurities were removed by ultrafiltration using MWCO 10 K membrane and resulting polymer (> 10 K fraction) was characterized by $^1$H-NMR spectrometer using $D_2O$ as a locking solvent. The chemical shifts of the PNiPAAm-OH were followed. PNiPAAm-OH $^1$H-NMR ($D_2O$, ppm, TMS): 3.61 ppm (polymer end, t, $HOCH_2CH_2S$-PNiPAAm), 3.83 ppm (**j** in Figure 2, -$CH(CH_3)_2$), 1.08 ppm (**i** in Figure 2, -$CH(CH_3)_2$), 1.19-2.58 ppm (polymer main chain -$CH$- and -$CH_2$-). Using the integration values of polymer end and peak **j**, number average molecular weight was calculated. The obtained $M_n$ value was 11,000 Da/mole. PNiPAAm-OH and mPEG-OH initiated ring-opening polymerization of ε-caprolactone were also confirmed by $^1$H-NMR spectra. The resulting block copolymer NMR spectra showed the coexistence of characteristic peaks of PCL block with PNiPAAm or PEG blocks. PNPCL $^1$H-NMR ($CDCl_3$, ppm, TMS): 3.92 ppm (**j**, -$CH(CH_3)_2$ in PNiPAAm), 1.08 ppm (**i**, -$CH(CH_3)_2$ in PNiPAAm), 1.19-2.58 ppm (PNiPAAm main chain -$CH$- and -$CH_2$-) 2.20 ppm (**d**, t, $OCOCH_2(CH_2)_4$ in PCL), 1.54 ppm (**e**, m, $OCOCH_2CH_2CH_2CH_2CH_2$ in PCL), 1.28 ppm (**f**, m, $OCOCH_2CH_2CH_2CH_2CH_2$ in PCL), and 3.96 ppm (**g**, t, $OCOCH_2CH_2CH_2CH_2CH_2$ in PCL). PEG-PCL $^1$H-NMR ($CDCl_3$, ppm, TMS): 3.27 ppm (**a**, s, $CH_3$-O in PEG end), 3.54 ppm (**b**, s, -$CH_2CH_2$-O in PEG), 2.20 ppm (**d**, t, $OCOCH_2(CH_2)_4$ in PCL), 1.54 ppm (**e**, m, $OCOCH_2CH_2CH_2CH_2CH_2$ in PCL), 1.28 ppm (**f**, m, $OCOCH_2CH_2CH_2CH_2CH_2$ in PCL), and 3.96 ppm (**g**, t, $OCOCH_2CH_2CH_2CH_2CH_2$ in PCL). The $M_n$ values and PCL block lengths were calculated based on integration values of each block copolymers and listed in Table I. PCL block lengths of 1,700 and 1,900 Da were calculated based on PNPCL and PEGCL $^1$H-NMR spectra, respectively. The block copolymer synthesis also confirmed by GPC chromatograms. The average molecular weights and polydispersity indexes of PEG, PNiPAAm, and block copolymers were listed in Table I.

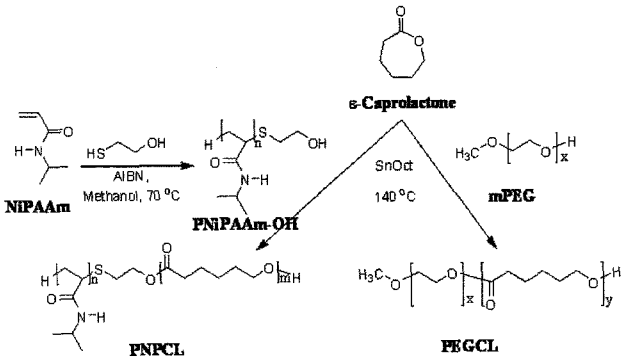


**Figure 1.** Synthetic scheme for PNPCL and PEGCL block copolymer.

**Characterization of Mixed Nanoparticles.** The amphiphilic block copolymers and hydrophobized water soluble polymers can self-aggregate to form micelle like self-

**Table I. Characterization of PNiPAAm, PNPCL and PEGCL Block Copolymer**

| Samples | HPL MW[a] | PCL MW[b] | PCL wt%[b] | $M_n$[b] | $M_n$[c] | PDI[c] |
|---|---|---|---|---|---|---|
| mPEG | 2 K | - | - | 2,000 | 1,690 | 1.20 |
| PEGCL | PEG, 2 K | 1,900 | 48.8 | 3,900 | 4,840 | 1.37 |
| PNiPAAm-OH | 11K | - | - | 11,000 | 11,400 | 2.10 |
| PNPCL | PNP, 11 K | 1,700 | 13.4 | 12,700 | 15,200 | 1.99 |

[a]Molecular weight of hydrophilic blocks. [b]Calculated based on $^1$H-NMR results. [c]GPC results (with polystyrene standards).

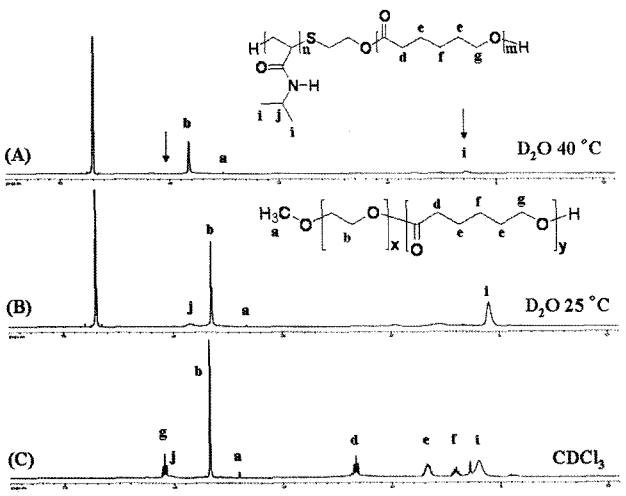


**Figure 2.** $^1$H-NMR spectra of M3 in (A) $D_2O$ (at 40 °C), (B) $D_2O$ (at 25 °C), and (C) $CDCl_3$, and peak assignment of the synthesized copolymer.

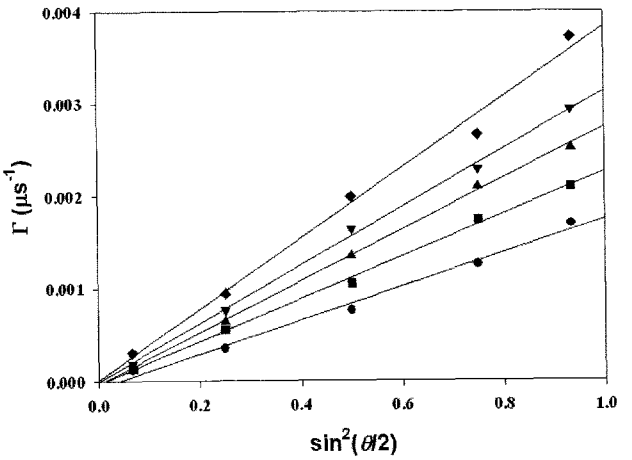


**Figure 3.** Relation ship between relaxation rate ($\Gamma$) versus scattering angle ($\sin^2(\theta/2)$) at 25 °C ([polymer solution] = 1.0 mg/mL). The regression lines indicate the best fit to the data according to eqs. (3) and (4) (●; M1, ■; M2, ▲; M3, ▼; M4, and ◆; M5).

aggregates in aqueous milieu. In case of PNPCL and PEGCL diblock copolymers, the formation of hydrophobic PCL domain in aqueous environment can easily be verified by $^1$H-NMR spectra with different locking solvents of $D_2O$ and $CDCl_3$. The results, as demonstrated in Figure 2 for 50/50 mixed aggregate (M3) of PNPCL and PEGCL, show that in $CDCl_3$, a nonselective solvent for the PNiPAAm, PEG, and PCL, the completed structural resolution of each constituent blocks were observed (Figure 2(C)). However, in $D_2O$, only the PEG and PNiPAAm signals were detected, mainly originated from the selective salvation of exterior hydrophilic corona chains through hydrogen bond formation with $D_2O$ (Figure 2(B)). The results clearly revealed that the PCL blocks in PNPCL and PEGCL block copolymers were self-associated into hydrophobic domain and remained in solid and/or semi-solid state, which resulted in the disappearance of PCL characteristic peaks in $D_2O$. Similar trends of $^1$H-NMR spectra are consistent with other amphiphilic block copolymer systems and hydrophobized polysaccharides.[2,5,51]

The mean diameter of PNPCL, PEGCL, and their mixed nanoparticles, prepared by solvent evaporation method and measured by DLS, were in the range of 190-260 nm (Table II), with slight increasing the particle size by increasing PNPCL portions. The increments of particle size with increasing PNPCL block content are mainly originated from the increment of bulky hydrophilic corona (MW of PNiPAAm is 11 K, that of PEG is 2 K). Furthermore, the fairly low polydispersity factors ($\mu_2/\Gamma^2$, 0.16-0.22), estimated by cumulant method, suggest that the nanoparticles showed narrow size distributions. The shapes of the self-aggregate were investigated by DLS with adopting different scattering angle. In case of spherical particles, there is no angular dependence of the translational diffusion coefficient ($D$).[46-48,52] As shown in Figure 3, the nanoparticles showed linear relationships between relaxation rates ($\Gamma$) and square of the scattering vector ($K$) according to;

$$\Gamma = DK^2 \tag{3}$$

$$K = 4\pi n_0 \sin(\theta/2)/\lambda_0 \tag{4}$$

**Table II. Characterizations of Mixed Nanoparticles by DSC, DLS, and Fluorescence Probe Method**

| Samples | PEGCL wt% | LCST[a] (°C) | LCST[b] (°C) | $d$ (nm)[c] | $d$ (nm)[d] | $\mu_2/\Gamma^{2}$[e] | $\chi_{PCL}^{f}$ | cac (mg/L) | $K_v^g$ (× $10^{-5}$) | $N_{PCL}^h$ |
|---|---|---|---|---|---|---|---|---|---|---|
| M1 | 0 | 34.5 | 35.1 | 259.6 | 264.3 | 0.21 | 0.134 | 5.33 | 5.00 | 7.84 |
| M2 | 25 | 34.6 | 35.2 | 231.3 | 239.7 | 0.17 | 0.223 | 3.02 | 5.14 | 8.07 |
| M3 | 50 | 35.3 | 36.1 | 230.0 | 234.6 | 0.16 | 0.311 | 2.71 | 5.38 | 8.46 |
| M4 | 75 | 36.1 | 36.4 | 204.6 | 230.8 | 0.21 | 0.400 | 2.10 | 5.94 | 10.55 |
| M5 | 100 | - | - | 191.4 | 195.3 | 0.22 | 0.488 | 1.43 | 6.60 | 13.99 |

[a]Lower critical solution temperature measured by transmittance change. [b]LCST measured by micro-DSC (endothermic peak point). [c]Particle size measured by DLS at 25 °C (Concentration of 1 mg/mL). [d]Particle size after thermal history (25 °C → 40 °C → 25 °C). [e]Polydispersity factor estimated by cumulant method. [f]PCL weight fraction calculated from $^1$H-NMR data. [g]Binding equilibrium constant of pyrene in water in the presence of the mixed nanoparticles. [h]Aggregation number of PCL blocks per on hydrophobic microdomain.

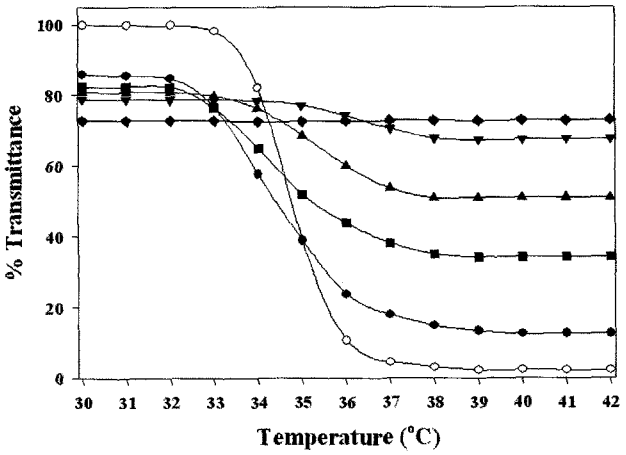


**Figure 4.** Measurement of the transmittance of PNiPAAm and mixed nanoparticles in PBS at $\lambda = 500$ nm (○; PNiPAAm-OH, ●; M1, ■; M2, ▲; M3, ▼; M4, and ◆; M5).

where $n_0$ is the solvent refractive index, $\lambda_0$ in the wavelength of incident light *in vacuo*, and $\theta$ is the scattering angle. The linear relationship due to the consistent translational diffusion coefficient with various detection angles, cause by undetectable rotational motion, represented that the self-aggregate in aqueous milieu are spherical.[46]

Poly(*N*-isopropylacrylamide) (PNiPAAm) is one of the most widely invested thermosensitive polymer with showing highly hydrated extended coil to globule transition upon heating (lower critical solution temperature, LCST). The transition resulted in the precipitation and/or sol to gel transformation of PNiPAAm or related copolymers. The transition phenomena can be easily characterized by optical property change (turbidimetry) of polymeric solution or *N*-isopropylacrylamide containing hydrogels, and the optical property change has been frequently employed for the criteria of the transition. PNiPAAm-OH and other mixed nanoparticles (M1-M4) showed optical property (transmittance at 500 nm) changes upon heating, as shown in Figure 4, and the transmittance changes were closely rely on PNiPAAm content. By increasing PNPCL content, the more sharp and dominant transmittance reductions were observed. From the Figure 4 results, the LCSTs were determined at a temperature with a half of the optical transmittance change between below and above the transitions, and the results were listed in Table II. The LCST was slightly decreased with increasing PNPCL content. While, M5, the self-aggregate consist with only PEGCL, did not show any transmittance change upon heating.

The LCST, coil to globule transition point, can be interpreted by thermodynamic view point. At the transition point, enthalpy change (heat of phase separation) is occurred due to the corresponding entropy change ($\Delta H = T\delta S$, since $\Delta G = 0$ for the phase transitions) and the thermodynamic event can be detected by micro-DSC. The endothermic peak points, obtained by micro-DSC measurement of the mixed aggregate solutions, were quietly closed with LCST values measured by transmittance change, and the results were listed in Table II.

The phase transition of PNiPAAm block in aqueous environment also affected the $^1$H-NMR spectra of the mixed nanoparticles. In microscopic point of view, the LCST can be interpreted as the temperature where solution to solid (or precipitate) and/or sol to gel transition occur. Therefore, the solution NMR spectra and resulting peaks originated form PNiPAAm block were severely affected by increasing temperature higher than its LCST. As shown in Figures 2(A) and 2(B), there are several differences, such as shifts of the characteristic peaks and reduction of PNiPAAm peaks, between NMR spectrum measured at 2 and 40 °C. Furthermore, significant reductions of integration ratio of peak **b** and **i** or **j** were occurred by the transition. The initial integration ratio of 0.235 (**j/b**, at 25 °C) and 1.089 (**i/b**) were reduced into 0.061 and 0.214, respectively, by measurement at 40 °C.

Shrinking of PNiPAAm corona by increasing temperature also affected the particle size of the mixed nanoparticles. Figure 5 illustrated the temperature dependent particle size variation of M1 (PNPCL), M3 (50/50 mixture of PNPCL and PEGCL), and M5 (PEGCL). In case of M1, significant decrease of the particle size was occurred by increasing temperature. Furthermore, at higher temperature than its LCST (at 40 °C), the M1 dispersion showed bimodal distribution of particles at 50 nm region and 200 nm region. The small sized particle may represent the shrunken particle by shrinking of outer PNiPAAm corona and the large sized particle may be formed by interparticular segregation of the shrunken particles. The reduction of particle size by increasing temperature was reduced by increasing PEGCL content. In case of M3, the particle size slightly decreased with increasing temperature, and maintained the particle size

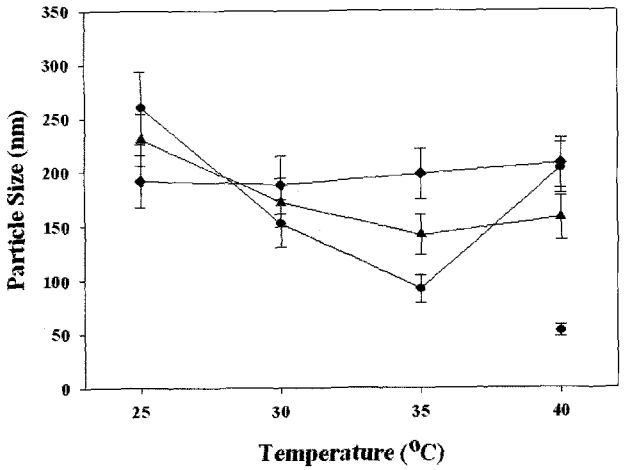


**Figure 5.** Particle size of mixed nanoparticles with increment temperature (●; M1, ▲; M3, and ◆; M5).

around 150 nm. Compared with M1, the segregation of shrunken particles did not observed with M3, mainly due to the interruption of particle-particle aggregation by hydrophilic PEG chains. While, there was no significant change of particle size on PEGCL self-aggregates (M5). Another interesting finding is reversible change of the particle size after thermal history (25 °C → 40 °C → 25 °C). Although the segregation of shrunken particles was occurred in PNPCL nanoparticles at higher temperature than its LCST, the segregates were returned to its original self-aggregates by decreasing temperature (Table II). Similar trends of particle size reduction, segregation, and reversible returning after thermal history have been reported with several *N*-isopropylacrylamide based amphiphilic copolymers.

To investigate microscopic self-aggregation behavior of the mixed nanoparticles in aqueous milieu, pyrene was used as a fluorescence probe. With exposure to polymeric self-aggregate aqueous solution, pyrene molecules preferably participate into inside or close to the hydrophobic microdomains of the self-aggregate rather than in aqueous phase. The localization, combined with strong fluorescence illumination of pyrene in a non-polar environment, shows the different photophysical characteristics depending on the concentration of self-aggregate forming materials.[2,53,54] Therefore, the self-aggregation behaviors of the mixed nanoparticles were investigated by using fluorescence excitation spectra of the mixed aggregate solutions with various concentrations, in the presence of $6.0 \times 10^{-7}$ M pyrene, and the results were illustrated in Figure 6. At low concentration ($c$ < cac), there are small or negligible changes of total fluorescence intensity and the shift of (0, 0) band at 335 nm. As increasing concentration remarkable increase of the total fluorescence intensity and a red shift of the (0, 0) band from 335 to 338 nm were observed. Figure 7 shows the intensity ratio

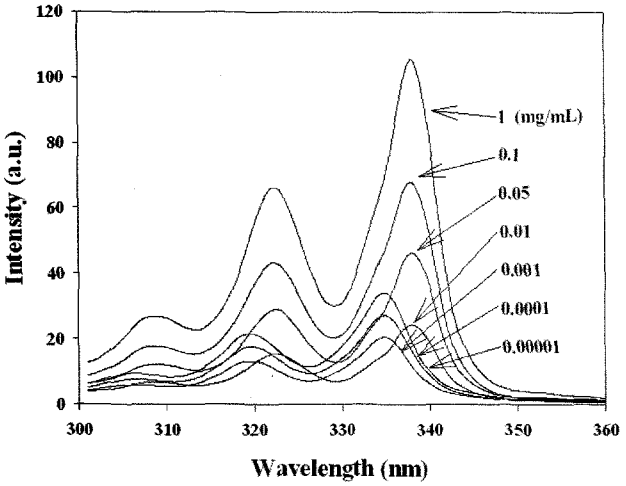


**Figure 6.** Pyrene excitation spectra ($[Py] = 6.0 \times 10^{-7}$ M) in mixed aggregate (M3) aqueous solutions (emission wavelength was 390 nm).

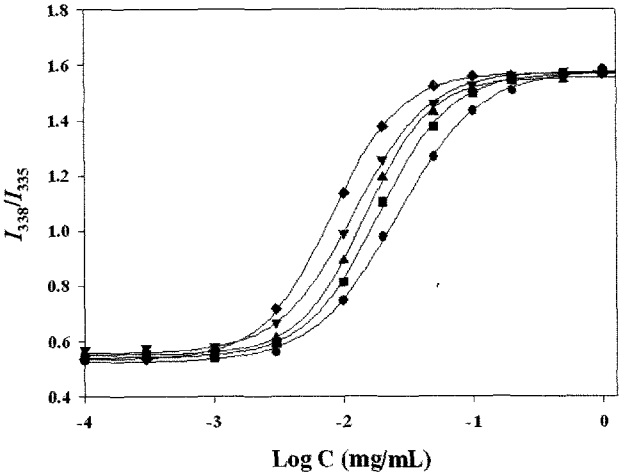


**Figure 7.** Plot of total fluorescence excitation intensity ratio ($I_{338}/I_{335}$) versus PNPCL and PEGCL block copolymers mixture concentrations (●; M1, ■; M2, ▲; M3, ▼; M4, and ◆; M5).

($I_{338}/I_{335}$) obtained by the pyrene excitation spectra versus the logarithm of the mixed aggregate concentrations. Based on the intensity ratio data, the cac values of the mixed nanoparticles were calculated by the crossover point at low concentration ranges. The cac values of the mixed nanoparticles were in the range of 1.43-5.33 mg/L with increasing the cac values with higher PNPCL content due to the decreased amount of hydrophobic PCL block in the mixed nanoparticles (Table II). The obtained cac values of the mixed nanoparticles were similar to the reported values of amphiphilic block copolymers and slightly lower than alkyl group end-capping PNIPAAms.[53,55,56]

The hydrophobic nature of interior microdomain of the mixed nanoparticles was investigated by estimating the pyrene equilibrium constant ($K_v$), originating from the localization of pyrene between aqueous and hydrophobic microdomain.[54] With assumption of simplified equilibrium state, the molar ratio of pyrene in the micellar phase to the water phase can be expressed as following equation:

$$[Py]_m/[Py]_w = K_v V_m/V_w \quad (5)$$

where $V_m$ and $V_w$ are the micellar and water phase volumes, respectively. In micellar association sensitive case, the eq * can be expressed as

$$[Py]_m/[Py]_w = K_v x_{PCL}(c - \text{cac})/1000\rho_{PCL} \quad (6)$$

where $x_{PCL}$ is the weight fraction of PCL block, $c$ is the concentration of the mixed nanoparticles and $\rho_{PCL}$ is the density of the inner core of self-aggregates (1.073-1.146 in Aldrich catalogue, adopt the average value of 1.10). In the intermediate range of the mixed aggregate concentrations, the $[Py]_m/[Py]_w$ values can be calculated by

$$[Py]_m/[Py]_w = (F - F_{min})/(F_{max} - F) \quad (7)$$

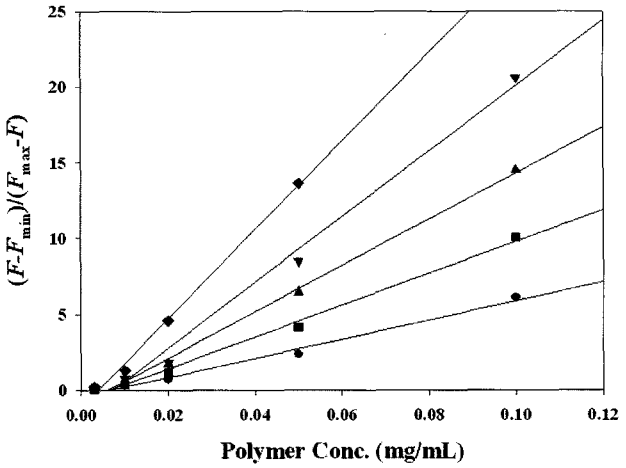


**Figure 8.** Plot of $(F - F_{min})/(F_{max} - F)$ versus PNPCL and PEGCL block copolymers mixture concentrations. Solid lines indicate the best fit to the data according to eq. (5) (●; M1, ■; M2, ▲; M3, ▼; M4, and ◆; M5).

where $F_{max}$ and $F_{min}$ are the intensity ratio ($I_{338}/I_{335}$) at high and low polymer concentration ranges, and $F$ in the intensity ration in the intermediate concentration range. Therefore, the equilibrium constant ($K_v$) values of pyrene in mixed aggregate solutions can be easily calculated from the slopes of $(F - F_{min})/(F_{max} - F)$ versus polymer concentration graph (Figure 8). As summarized in Table II, the $K_v$ values were in the range of 5.0-6.6 × $10^5$. Slightly increasing the $K_v$ values with increasing PEGCL content might originated the slightly longer PCL block length in PEGCL (1,900 Da) than PNPCL (1,700 Da) which resulted in the increased hydrophobicity in PEGCL rich mixed nanoparticles. Compared to the mixed nanoparticles, other amphiphilic copolymers such as PEG-PLLA, poly(2-ethyl-2-oxazoline)-PCL, and PVP-PCL block copolymers showed similar $K_v$ values (1-6 × $10^5$), depending on the hydrophilic-hydrophobic balance.[39,53]

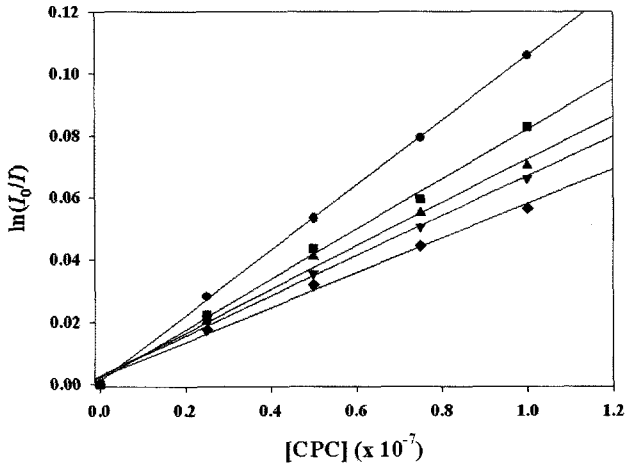


**Figure 9.** Plot of fluorescence intensity $\ln(I_0/I)$ versus CPC quencher concentration (●; M1, ■; M2, ▲; M3, ▼; M4, and ◆; M5).

To determine the aggregation number of PCL chains in a hydrophobic microdomain, the mixed nanoparticles were investigated by using a fluorescence quenching method with various quencher concentrations.[49,50] As shown in Figure 9, the $\ln(I_0/I)$ versus CPC concentration plots showed linear relationships and aggregation numbers of PCL blocks can be calculated using slope of the straight line using eq. (2). The obtained aggregation numbers of PCL blocks in a hydrophobic microdomain were in the range of 7-14, depending the mixed aggregate compositions as summarized in Table II. The results revealed that the mixed nanoparticles with longer hydrophilic PNiPAAm blocks (M1, $N_{PCL}$ = 7.84) consisted with relatively small number of PCL block to form a hydrophobic microdomain than block copolymer having shorter PEG block (M5, $N_{PCL}$ = 13.99), due to sterical difficulty of intermolecular hydrophobic aggregation of PCL blocks.

**Drug Loading and Release Studies.** As listed in Table III, mixed nanoparticles showed excellent characteristics for drug carriers owing to their high drug loading efficiencies (78.8-97.7%) and drug contents (13.6-16.4%). Drug contents and loading efficiency increased with increment of PEGCL portion because of increasing of hydrophobic core capacity and hydrophobicity (Table II).

To investigate the effect of PNiPAAm block on drug release behaviors, the drug release tests were performed at two different temperature of 25 °C (below PNiPAAm LCST) and 37 °C (above PNiPAAm LCST) with three different CNZ loaded mixed nanoparticles. As illustrated in Figure 10, the CNZ loaded M1 showed well-developed sustained drug release patterns (at 37 °C). In case of 25 °C release tests (Figure 10(A)), the drug releases were completed (> 95% release) at 10 and 14 days after incubation from M1 and M3 nanoparticles, respectively. The release tests performed at 37 °C showed reverse drug release patterns (Figure 10(B)). The effect of PNiPAAm hydrogel layers on the nanoparticle surface by temperature phase transition also affected drug release patterns (at 37 °C). Owing to the increase of hydrophobicity of the PNPCL aggregate shell compartments, the sustained drug release patterns were increased. Whereas,

**Table III. Characterization of Clonazepam Loaded Mixed Nanoparticles**

| Samples | Polymer (mg) | Drug (mg) | Drug Content (%) | Loading Efficiency (%) |
|---|---|---|---|---|
| M1 | 20 | 4 | 13.6 | 78.8 |
| M2 | 20 | 4 | 15.7 | 93.0 |
| M3 | 20 | 4 | 16.1 | 96.1 |
| M4 | 20 | 4 | 16.3 | 97.7 |
| M5 | 20 | 4 | 16.4 | 97.7 |

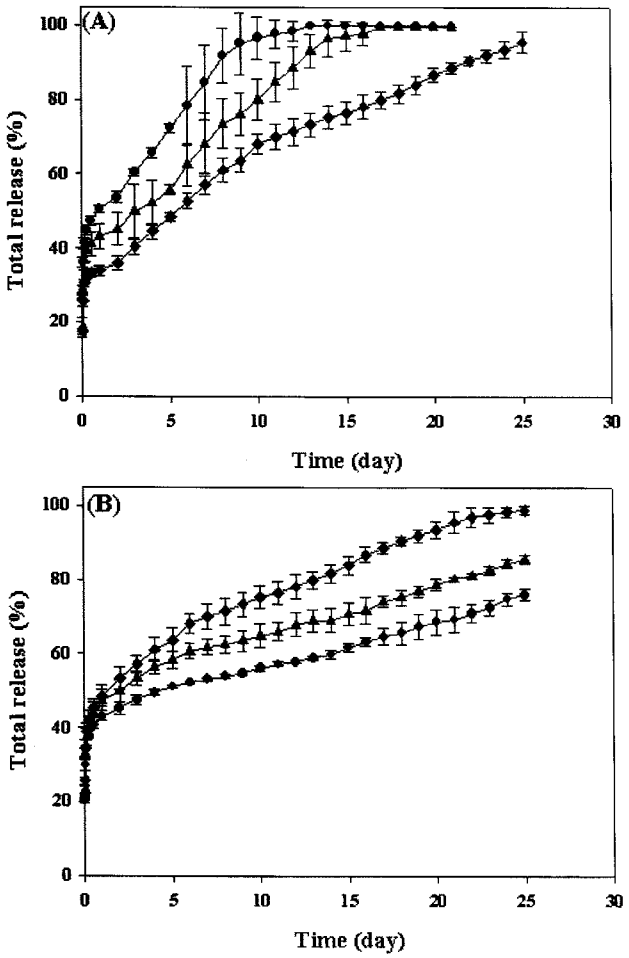


**Figure 10.** Total drug (clonazepam) release behavior from nanoparticles at 25 °C (A) and 37 °C (B) (●; M1, ▲; M3, and ◆; M5).

drug release patterns of M5 (without PNiPAAm block on nanoparticle) was independence of temperature. Therefore, it is possible to conclude that the formation of PNiPAAm hydrogel layer might be act as additional diffusion barrier for the drug release.

## Conclusions

In this study, thermosensitive nanoparticles were prepared by self assembly of two different poly(ε-caprolactone) based block copolymers of poly(*N*-isopropylacrylamide)-*b*-poly(ε-caprolactone) (PNPCL) and poly(ethylene glycol)-*b*-poly(ε-caprolactone) (PEGCL). The self-aggregation and thermosensitive behaviors of the mixed nanoparticles (with different PNPCL content) were investigated by using $^1$H-NMR, turbidimetry, differential scanning microcalorimetry (micro-DSC), dynamic light scattering (DLS), and fluorescence spectroscopy. The copolymer mixtures (mixed nanoparticles, M1-M5, with different PNPCL content) formed nano-sized self-aggregates in aqueous environment by intra- and/or intermolecular association of hydrophobic PCL chains. The microscopic investigation of the mixed nanoparticles revealed that the critical aggregation concentration (CAC), the partition equilibrium constants ($K_v$) of pyrene, and the aggregation number of PCL chain per one hydrophobic microdomain were varied by compositions of the mixed nanoparticles. Furthermore, the PNPCL containing mixed nanoparticles showed phase transition behavior, originated by coil to globule transition of PNiPAAm block upon heating, which resulted in the turbidity change, endothermic heat exchange, and reduction of particle size upon heating. Also, we confirmed that PNiPAAm of thermosensitive aggregate became hydrophobic and forms hydro-gel layer on surface of polymeric nanoparticles above the LCST and this layer played a high potential for sustained release of drug due to hydro-gel layer on surface of nanoparticles.

Based on these results, it is possible to introduction of mixed nanoparticles composed to PNPCL and PEGCL block copolymers into various biomedical fields such as drug delivery.

**Acknowledgement.** This study was supported by Technology in Korea, and Korea Sanhak Foundation (2006).

## References

(1) J. A. Hubbell, *Science*, **300**, 595 (2003).
(2) S. Kwon, J. H. Park, H. Chung, I. C. Kwon, S. Y. Jeong, and I. Kim, *Langmuir*, **19**, 10188 (2003).
(3) K. Kataoka, A. Harada, and Y. Nagasaki, *Adv. Drug Deliver. Rev.*, **47**, 113 (2001).
(4) K. Y. Lee, W. H. Jo, I. C. Kwon, Y. Kim, and S. Y. Jeong, *Macromolecules*, **31**, 378 (1998).
(5) J. S. Hrkach, M. T. Peracchia, A. Domb, N. Lotan, and R. Langer, *Biomaterials*, **18**, 27 (1997).
(6) T. Riley, S. Stolnik, C. R. Heald, C. D. Xiong, M. C. Garnett, L. Illum, S. S. Davis, S. C. Purkiss, R. J. Barlow, and P. R. Gellert, *Langmuir*, **17**, 3168 (2001).
(7) G. Ruan and S. S. Feng, *Biomaterials*, **24**, 5037 (2003).
(8) C. Brus, H. Petersen, A. Aigner, F. Caubayko, and T. Kissel, *Bioconjug. Chem.*, **15**, 677 (2004).
(9) Y. Yamamoto, Y. Nagasaki, Y. Kato, Y. Sugiyama, and K. Kataoka, *J. Control. Release*, **77**, 27 (2001).
(10) J. P. Xu, J. Ji, W. D. Chen, and J. C. Shen, *J. Control. Release*, **107**, 502 (2005).
(11) S. S. Venkatraman, P. Jie, F. Min, B. Y. Freddy, and G. Leong-Huat, *Int. J. Pharm.*, **298**, 219 (2005).
(12) P. Opanasopit, M. Yokoyama, M. Watanabe, K. Kawano, Y. Maitani, and T. Okano, *Pharm. Res.*, **21**, 2001 (2004).
(13) F. Zeng, J. Liu, and C. Allen, *Biomacromolecules*, **5**, 1810 (2004).
(14) H. Cho, D. Chung, and A. Jeongho, *Biomaterials*, **25**, 3733 (2004).
(15) S. Zhou, X. Deng, and H. Yang, *Biomaterials*, **24**, 3563 (2003).

(16) M. F. Francis, M. Piredda, and F. M. Winnik, *J. Control. Release*, **93**, 55 (2003).
(17) H. S. Yoo, J. E. Lee, H. Chung, I. C. Kwon, and S. Y. Jeong, *J. Control. Release*, **103**, 235 (2005).
(18) S. W. Jung, Y. I. Jeong, and S. H. Kim, *Int. J. Pharm.*, **254**, 109 (2003).
(19) K. Akiyoshi, S. Kobayashi, S. Shichibe, D. Mix, M. Baudys, S. W. Kim, and J. Sunamoto, *J. Control. Release*, **54**, 313 (1998).
(20) I. C. Kwon, Y. H. Kim, and S. Y. Jeong, *Macromolecules*, **31**, 378 (1998).
(21) K. Kataoka, G. S. Kwon, M. Yokoyama, T. Okano, and Y. Sakurai, *J. Control. Release*, **24**, 119 (1993).
(22) Y. Matsumura and H. Maeda, *Cancer Res.*, **46**, 6387 (1986).
(23) G. Kwon, M. Naito, M. Yokoyama, T. Okano, Y. Sakurai, and K. Kataoka, *J. Control. Release*, **48**, 195 (1997).
(24) X. Z. Zhang, F. J. Wang, and C. C. Chu, *J. Mater. Sci. Mater. Med.*, **14**, 451 (2003).
(25) X. Zhang, D. Wu, and C. C. Chu, *Biomaterials*, **25**, 4719 (2004).
(26) L. Verestiu, C. Ivanov, E. Barbu, and J. Tsibouklis, *Int. J. Pharm.*, **269**, 185 (2004).
(27) S. Kim and K. E. Healy, *Biomacromolecules*, **4**, 1214 (2003).
(28) K. Makino, J. Hiyoshi, and H. Ohshima, *Colloid Surface B*, **20**, 341 (2001).
(29) B. Jeong, Y. H. Bae, D. S. Lee, and S. W. Kim, *Nature*, **388**, 860 (1997).
(30) B. Jeong, S. W. Kim, and Y. H. Bae, *Adv. Drug Deliver. Rev.*, **54**, 37 ( 2002).
(31) B. Vernon, S. W. Kim, and Y. H. Bae, *J. Biomed. Mater. Res.*, **51**, 69 (2000).
(32) D. Neradovic, O. Soga, C. F. Van Nostrum, and W. E. Hennink, *Biomaterials*, **25**, 2409 (2004).
(33) F. Kohori, K. Sakai, T. Aoyagi, M. Yokoyama, Y. Sakurai, and T. Okano, *J. Control. Release*, **55**, 87 (1998).
(34) K. Uchida, K. Sakai, E. Ito, O. H. Kwon, A. Kikuchi, M. Yamato, and T. Okano, *Biomaterials*, **21**, 923 (2000).
(35) J. E. Chung, M. Yokoyama, T. Aoyagi, Y. Sakurai, and T. Okano, *J. Control. Release*, **53**, 119 (1998).
(36) J. E. Chung, M. Yokoyama, M. Yamato, T. Aoyagi, Y. Sakurai, and T. Okano, *J. Control. Release*, **62**, 115 (1999).
(37) F. Kohori, K. Sakai, T. Aoyagi, M. Yokoyama, M. Yamato, Y. Sakurai, and T. Okano, *Colloid Surface B*, **16**, 19 (1999).
(38) F. Kohori, M. Yokoyama, K. Sakai, and T. Okano, *J. Control. Release*, **78**, 155 (2002).
(39) S. C. Lee, Y. Chang, J. Yoon, C. Kim, I. C. Kwon, Y. Kim, and S. Y. Jeong, *Macromolecules*, **32**, 1847 (1999).
(40) M. Yuan, Y. Wang, X. Li, C. Xiong, and X. Deng, *Macromolecules*, **33**, 1613 (2000).
(41) G. Zhang, A. Niu, S. Peng, M. Jiang, Y. Tu, M. Li, and C. Wu, *Acc. Chem. Res.*, **34**, 249 (2001).
(42) A. Albertsson and I. K. Varma, *Biomacromolecules*, **4**, 1466 (2003).
(43) B. S. Lele and J.-C. Leroux, *Macromolecules*, **35**, 6714 (2002).
(44) P. L. Soo, L. Luo, D. Maysinger, and A. Eisenberg, *Langmuir*, **18**, 9996 (2002).
(45) A. Harada and K. Kataoka, *Macromolecules*, **28**, 5294 (1995).
(46) A. Harada and K. Kataoka, *Macromolecules*, **31**, 288 (1998).
(47) K. Akiyoshi, S. Deguchi, H. Tajima, T. Nishikawa, and J. Sunamoto, *Macromolecules*, **30**, 857 (1997).
(48) K. Y. Lee, W. H. Jo, I. C. Kwon, Y. Kim, and S. Y. Jeong, *Langmuir*, **14**, 2329 (1998).
(49) S. Kwon, J. H. Park, H. Chung, I. C. Kwon, S. Y. Jeong, and I.-S. Kim, *Langmuir*, **19**, 10188 (2003).
(50) N. J. Turro and A. Yekta, *J. Am. Chem. Soc.*, **100**, 5951 (1978).
(51) C. R. Heald, S. Stolnik, K. S. Kujawinski, C. De Matteis, M. C. Garnett, L. Illum, S. S. Davis, S. C. Purkiss, R. J. Barlow, and P. R. Gellert, *Langmuir*, **18**, 3669 (2002).
(52) E. Alami, M. Almgren, W. Brown, and J. Francois, *Macromolecules*, **29**, 2229 (1996).
(53) S. K. Han, K. Na, and Y. H. Bae, *Colloid Surface A*, **214**, 49 (2003).
(54) M. Wilhelm, C. L. Zhao, Y. Wang, R. Xu, M. A. Winnik, J. L. Mura, G. M. Riess, and D. Croucher, *Macromolecules*, **24**, 1033 (1991).
(55) S. C. Lee, Y. Chang, J. S. Yoon, C. Kim, I. C. Kwon, Y. H. Kim, and S. Y. Jeong, *Macromolecules*, **32**, 1847 (1998).
(56) B. S. Lele and J. C. Leroux, *Macromolecules*, **35**, 6714 (2002).